

## Review



**Cite this article:** Wells PS. 2015 The upgraded ATLAS and CMS detectors and their physics capabilities. *Phil. Trans. R. Soc. A* **373**: 20140046.  
<http://dx.doi.org/10.1098/rsta.2014.0046>

One contribution of 12 to a Discussion Meeting Issue 'Before, behind and beyond the discovery of the Higgs boson'.

### Subject Areas:

high energy physics, particle physics

### Keywords:

CERN, LHC, ATLAS, CMS, Higgs

### Author for correspondence:

Pippa S. Wells

e-mail: [pippa.wells@cern.ch](mailto:pippa.wells@cern.ch)

# The upgraded ATLAS and CMS detectors and their physics capabilities

Pippa S. Wells

CERN, Geneva 1211, Switzerland

The update of the European Strategy for Particle Physics from 2013 states that Europe's top priority should be the exploitation of the full potential of the LHC, including the high-luminosity upgrade of the machine and detectors with a view to collecting 10 times more data than in the initial design. The plans for upgrading the ATLAS and CMS detectors so as to maintain their performance and meet the challenges of increasing luminosity are presented here. A cornerstone of the physics programme is to measure the properties of the 125 GeV Higgs boson with the highest possible precision, to test its consistency with the Standard Model. The high-luminosity data will allow precise measurements of the dominant production and decay modes, and offer the possibility of observing rare modes including Higgs boson pair production. Direct and indirect searches for additional Higgs bosons beyond the Standard Model will also continue.

## 1. Introduction: the LHC timeline

Moving beyond the Higgs boson discovery, the Large Hadron Collider (LHC) has a long future. The update of the European Strategy for Particle Physics was formally adopted by the CERN council at the European Commission in Brussels on 30 May 2013 [1] and states that:

The discovery of the Higgs boson is the start of a major programme of work to measure this particle's properties with the highest possible precision for testing the validity of the Standard Model and to search for further new physics at the energy frontier. The LHC is in a unique position to pursue this programme.

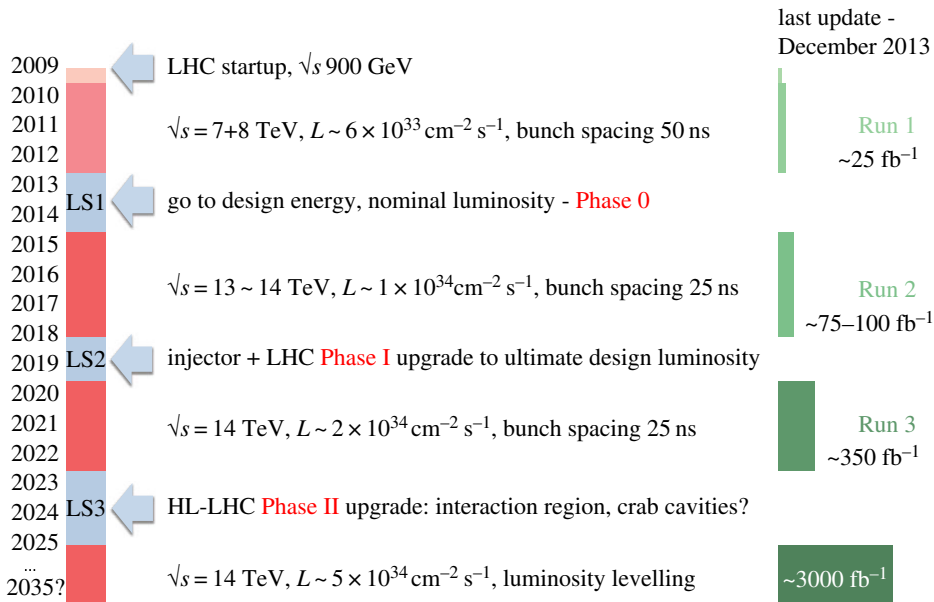


**Figure 1.** The LHC roadmap to achieve full potential with 10 times the original design integrated luminosity from the Phase II upgrade to the HL-LHC. (Online version in colour.)

Europe's top priority should be the exploitation of the full potential of the LHC, including the high-luminosity upgrade of the machine and detectors with a view to collecting ten times more data than in the initial design, by around 2030. This upgrade programme will also provide further exciting opportunities for the study of flavour physics and the quark-gluon plasma.

The LHC timeline to achieve this is outlined in figure 1. The success of Run 1 has been widely reported by other speakers at this meeting. At present, the accelerator is being refurbished so as to resume running in 2015 at close to design energy, and with nominal luminosity. After a second long shutdown starting in 2018, further improvements will allow a doubling of the luminosity, aiming to deliver in total the original target of approximately  $300 \text{ fb}^{-1}$ . At this point, the final focus magnets which squeeze the beams to a tight spot at the interaction regions are expected to suffer radiation damage and would need to be replaced. This gives the opportunity to upgrade the machine to the high luminosity LHC (HL-LHC), allowing at least five times the nominal instantaneous luminosity to be delivered after the third long shutdown and an integrated luminosity of  $3000 \text{ fb}^{-1}$  to be accumulated, 10 times the original design.

## 2. ATLAS and CMS detector upgrades

The increase in both the integrated and the instantaneous luminosities have an impact on the detectors. The integrated luminosity implies an increasing radiation dose; after the original design total luminosity is delivered, some parts will need replacement. In addition, the higher instantaneous luminosity means many more events occur in the same bunch crossing. This high 'pile-up' means that finer granularity detector layers are needed to separate the particles in the event. In order to keep high efficiency for picking out the most interesting events on the fly while rejecting background events, higher granularity and/or faster electronics will also be needed to pass more information to the trigger systems. The upgrade programmes follow the steady increase in luminosity and are denoted as Phase 0, I and II. In addition to the more obvious changes to the detectors, a continuous consolidation of support systems such as cooling or power

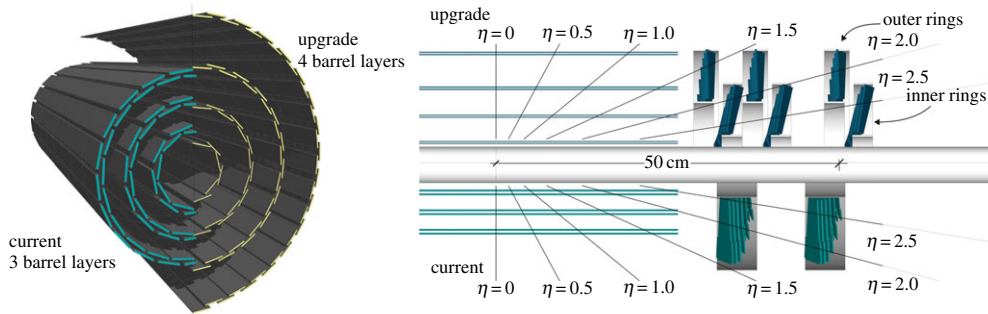


**Figure 2.** Two different views of the current and upgraded CMS pixel detector, showing how an extra layer of sensors will fit into both the barrel and endcap regions. (Online version in colour.)

supplies has to be carried out. In a nutshell, detector upgrades are planned so as to maintain or improve on the present performance as the instantaneous luminosity increases. A few illustrative examples are given here.

### (a) Phase 0: pixel detector improvements

The innermost layers of the tracking detectors are silicon pixel detectors, which allow the vertex or point of origin of charged particles to be very precisely measured. To improve the tracking capability in the presence of higher pile-up than the original design, both ATLAS and CMS are modifying their pixel detectors as one of the Phase 0 upgrades. In the case of ATLAS, a smaller radius beam pipe will allow an additional innermost layer of pixel sensors to be added during the present long shutdown [2]. This ‘insertable b-layer’ will have smaller pixels; the existing layers have  $50 \times 400 \mu\text{m}$  pixels, while the new layer has  $50 \times 250 \mu\text{m}$  and a new readout chip to match. The improved track and vertex measurements also help in tagging heavy  $b$ -quarks and  $\tau$ -leptons, which are particularly important for Higgs boson studies.

The CMS experiment will also add an extra pixel layer, but by a full replacement of the present pixel detector [3]. The current and upgraded layouts are compared in figure 2. The upgrade will have a new read out chip to prevent data loss, and thanks to improvements in cooling and powering will have less material in total than the present detector, despite the extra layer. A smaller radius beam pipe is being installed during the present shutdown so as to be able to install the new pixel detector in an extended end of year shutdown in 2016–2017. The new detector is expected to reduce background from light-flavour jets misidentified as  $b$ -quark jets by a factor of about five for the same  $b$ -tagging efficiency.

### (b) Phase I: upgrades

ATLAS plan to replace the so-called ‘small’ wheels of the muon spectrometer in the second long shutdown [4]. The small wheels are a mere 10 m in diameter, compared with the 25 m big wheels. The new, higher granularity detector technologies to be used will maintain good momentum resolution in the presence of pile-up and give a faster signal allowing a track segment to be used in the trigger. The present trigger is dominated by fake muons in the region of the muon wheels, as shown in figure 3*a* (hatched area). When the triggered segment is required to line up with a muon candidate which is well reconstructed offline, consisting of both an inner detector track and muon segment, the rate is much reduced (shaded area). Figure 3*b* illustrates how a muon originating from the interaction point gives track segments that line up in the small and big wheels (A), while fake muons (B or C) do not.

The readout devices of the CMS hadron calorimeter need to be replaced. As well as fixing some readout noise issues, the new devices will allow more segmentation in depth [5]. This is

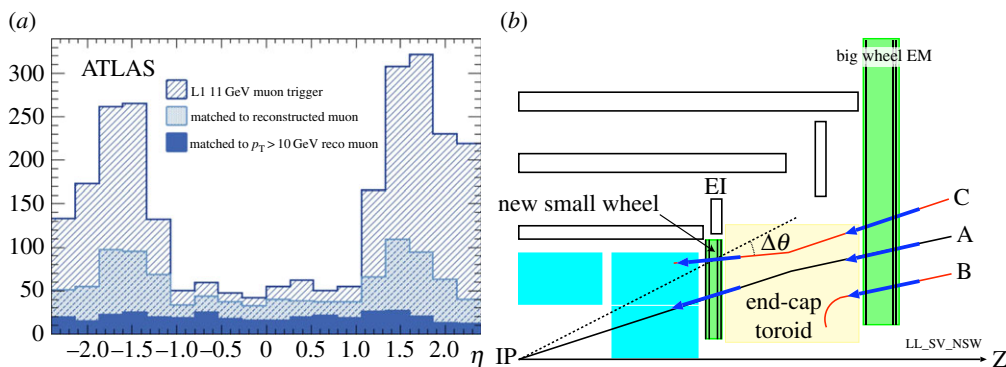


**Figure 3.** As explained in the text, the rate of muon triggers in the present ATLAS detectors is dominated by fake muons in the higher  $|\eta|$  regions (a). These can be rejected by matching to a track segment in the small wheel (b). (Online version in colour.)

particularly important to maintain high efficiency for particle identification in a high pile-up environment. The hit occupancy in the hadron calorimeter drops by two orders of magnitude from the front layers of scintillator directly surrounding the electromagnetic calorimeter to the rear layers that sit in front of the muon systems. Hadron showers from a high energy particle that are measured at multiple depths can be distinguished from the deposits made by low energy particles in pile-up events.

### (c) Phase II: to exploit the high luminosity LHC

Moving to the HL-LHC, the central trackers of both experiments will have started to suffer from radiation damage, and the occupancies in the presence of five times the nominal instantaneous luminosity would make pattern recognition too difficult. Both experiments plan to replace the trackers with higher granularity silicon sensors—pixels and microstrips. For ATLAS, the baseline Phase II tracker will give better  $b$ -tagging performance and muon momentum resolution than the present tracker [6]. This is illustrated in figure 4. The ATLAS Phase I calorimeter and muon system upgrades are all designed to be compatible with Phase II operation. Additional improvements to the readout electronics will be made to be able to pass more information to the trigger. An extension of the coverage in the forward region, i.e. at angles closer to the beam line, is also being considered.

The CMS Phase II plans are also exploring an extension into the forward region [7]. A possible layout for the tracker is shown in figure 5, with additional pixel discs to measure tracks close to the beam pipe. The endcap and forward calorimeters would also be replaced, and the muon chamber coverage could be extended to match the increased tracker coverage. The benefits of such an extension are shown in figure 6 [8]. The signal acceptance for Higgs boson decays to four muons is increased by approximately 40%.

## 3. Prospects for measurements of the Higgs boson

The prospects for Higgs boson measurements have been compared for the  $300 \text{ fb}^{-1}$  sample originally proposed for the LHC, and the high luminosity extension, HL-LHC, delivering a total of  $3000 \text{ fb}^{-1}$ . A major goal is to measure all the possible production and decay modes [9,10]. The dominant processes can be measured precisely, and first observations could be made of rare processes. These measurements are then interpreted in terms of Higgs boson couplings to other particles. There are also direct searches for additional Higgs bosons, and indirect constraints on new physics processes which can be inferred from the coupling measurements. By contrast, the mass and width measurements will be very difficult to improve with the HL-LHC running.

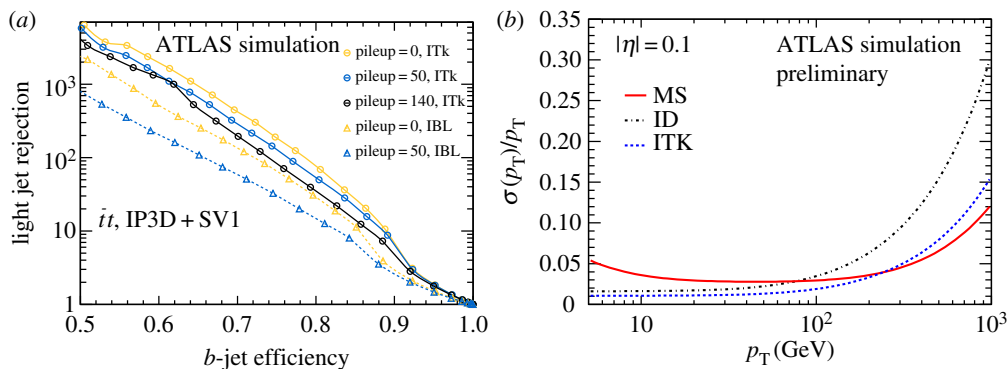


**Figure 4.** The ATLAS light jet rejection as a function of  $b$ -tagging efficiency (a). The dotted lines show the performance of the present tracker with the additional pixel layer, IBL and the solid lines show that the Phase II upgrade will give better performance even in the presence of higher pile-up. The muon momentum resolution will also be improved (b). The curves compare the resolution of the muon spectrometer (MS), the present tracker (ID) and the Phase II upgrade (ITK). (Online version in colour.)

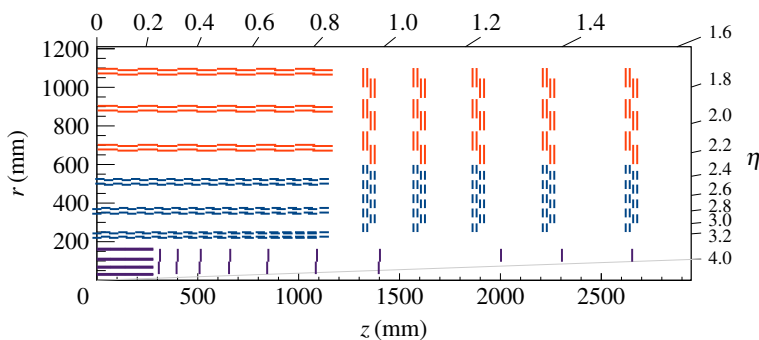


**Figure 5.** A quadrant of the CMS Phase II tracker layout, with an extension to  $\eta = 4$  using pixel discs. (Online version in colour.)

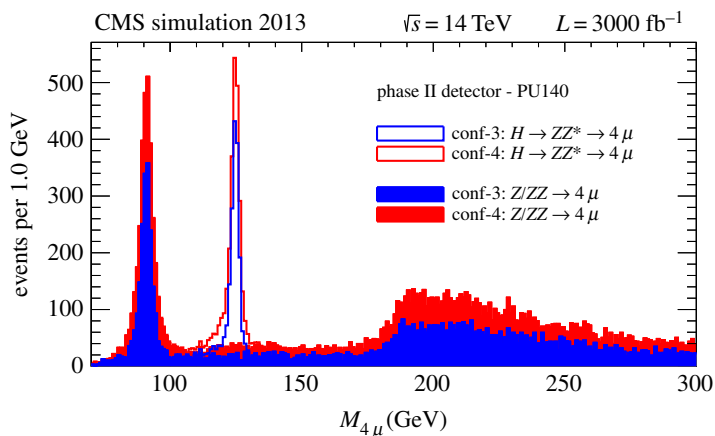


**Figure 6.** The rate of  $H \rightarrow 4\mu$  events (open histograms) and irreducible  $Z/ZZ \rightarrow 4\mu$  background (solid) for two CMS upgrade configurations, covering to  $|\eta| < 2.5$  (dark grey/blue) or 4.0 (light grey/red). (Online version in colour.)

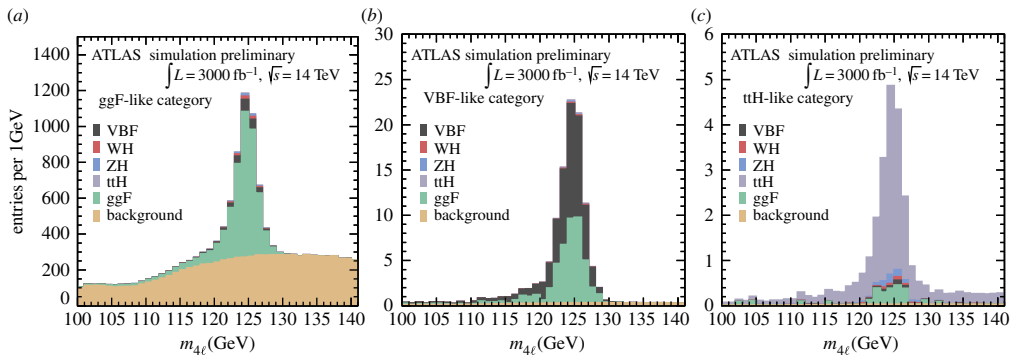


**Figure 7.** (a–c) ATLAS  $H \rightarrow ZZ \rightarrow 4\ell$  samples enriched in ggF, VBF or ttH production. (Online version in colour.)

**Table 1.** The number of  $H \rightarrow ZZ \rightarrow 4\ell$  signal events predicted by ATLAS in  $3000 \text{ fb}^{-1}$  of HL-LHC data.

signal events	ggH	VBF	ttH	WH	ZH
$3000 \text{ fb}^{-1}$	3800	97	35	67	5.7

A direct measurement of the expected very narrow width is limited by the detector resolutions. However, indirect constraints from interference effects may be possible. Although the dominant spin and parity will already be very well established, strong constraints on any admixture of non-standard contributions can be made.

The HL-LHC is a Higgs boson factory, with over 100 million Standard Model Higgs bosons produced in  $3000 \text{ fb}^{-1}$ , and over 1 million by each of the main production mechanisms, in proportion to the production cross sections. These are spread over many decay modes, according to the decay branching ratios. There could be 20 thousand  $H \rightarrow ZZ \rightarrow 4\ell$  events, 400 thousand  $H \rightarrow \gamma\gamma$ , but only 50 of the very rare mode  $H \rightarrow J/\psi\gamma$ , which might give a way of measuring the coupling to charm quarks.

To account for the detector performance, the ATLAS predictions use detector response functions based on full simulation of the Phase I detector (including the new pixel layer) and a typical pile-up of 50, and of the Phase II detector with pile-up of 140 [11]. The results are presented with and without theoretical uncertainties included. The CMS results are extrapolations from the present (Run 1) 7 and 8 TeV analyses, assuming that the detector upgrades maintain the detector performance. In scenario 1, experimental systematic and theoretical uncertainties are unchanged, and statistical uncertainties scale with the integrated luminosity as  $1/\sqrt{\mathcal{L}}$ . In scenario 2, statistical and experimental systematic uncertainties scale with  $1/\sqrt{\mathcal{L}}$ , while theoretical uncertainties are assumed to be reduced by a factor 2. In other words, both ATLAS and CMS include systematic uncertainties, but making different assumptions on possible improvements in the detectors, in the algorithms to identify final state particles, and in theoretical inputs.

## (a) Typical measurements

The decay of the Higgs boson to four leptons,  $H \rightarrow ZZ \rightarrow 4\ell$ , was one of the first discovery channels. This high purity signal will allow all five of the main production modes to be measured with  $3000 \text{ fb}^{-1}$ . The numbers of signal events from gluon–gluon fusion (ggF), vector boson fusion (VBF), and from associated production with a  $t\bar{t}$  pair (ttH) or a W or Z boson (WH or ZH) are given in table 1. VBF and ttH events are identified from increasing numbers of additional jets in the event, while WH and ZH events have additional leptons. The signal distributions for the first three modes are shown in figure 7.

Examples of rare processes are illustrated in figure 8. The decay  $H \rightarrow \mu\mu$  gives the first opportunity to measure the Higgs boson decaying to second generation fermions. Both ATLAS

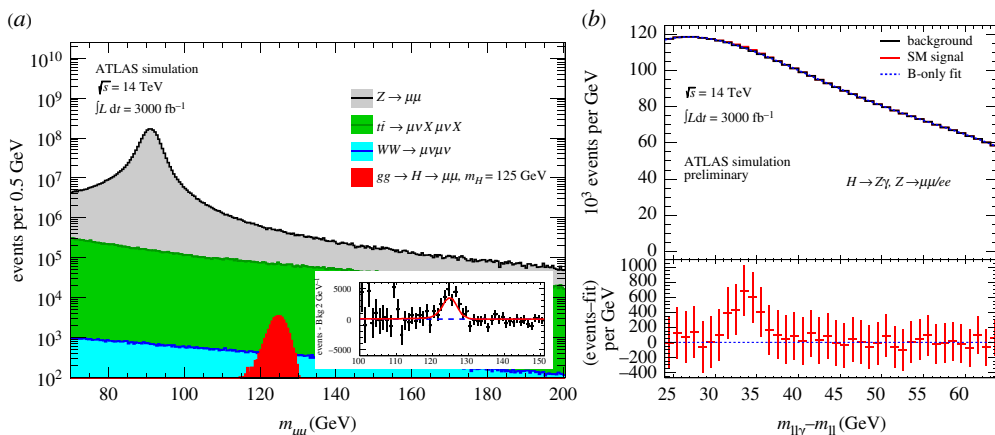


**Figure 8.** Predicted signals with  $3000 \text{ fb}^{-1}$  for the rare processes  $H \rightarrow \mu\mu$  (a) and  $H \rightarrow Z\gamma$  (b). (Online version in colour.)

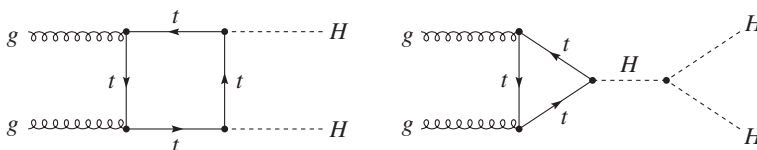


**Figure 9.** Higgs boson pair production processes. The diagram on the right includes the direct triple Higgs coupling.

**Table 2.** The number of Higgs pair signal events in  $3000 \text{ fb}^{-1}$  of HL-LHC data.

$HH$ signal	$bbWW$	$bb\tau\tau$	$WWWW$	$\gamma\gamma bb$	$\gamma\gamma\gamma\gamma$
$3000 \text{ fb}^{-1}$	30 000	9000	6000	320	1

and CMS expect to be able to observe this with more than  $5\sigma$  significance in  $3000 \text{ fb}^{-1}$ , which would allow the coupling to be determined to 10–20%. ATLAS also predict that about 30 signal events could be observed in the  $t\bar{t}H$  production mode, with  $H \rightarrow \mu\mu$ . The decay  $H \rightarrow Z\gamma$  proceeds via a loop, like the well established mode  $H \rightarrow \gamma\gamma$ , and in contrast to  $H \rightarrow ZZ$ , where there is a direct coupling. Despite the challenging background, a measurement should be possible at the HL-LHC.

The rate of Higgs boson pair production must be measured to determine the strength of the self-coupling of Higgs bosons. The two main types of process to produce two Higgs bosons are illustrated in figure 9. The diagram on the right involves the direct coupling of three Higgs bosons, which is an integral part of the Higgs sector of the Standard Model. However, there is a destructive interference between the two processes, i.e. if the Higgs self-coupling increases the overall rate should decrease. With the Standard Model value, the production cross section is  $34 \text{ fb}$ , resulting in the signal rates in table 2. If the coupling were zero, the production cross section would approximately double ( $71 \text{ fb}$ ), and if the coupling doubles, the cross-section halves ( $16 \text{ fb}$ ). Ongoing studies suggest that Higgs pair production could be observed at the HL-LHC, but this is a challenging analysis.

## (b) Signal strength precision

The predicted uncertainty in the measurement of the signal strength for various Higgs boson production and decay modes is shown in figures 10 and 11 for ATLAS and CMS, respectively.



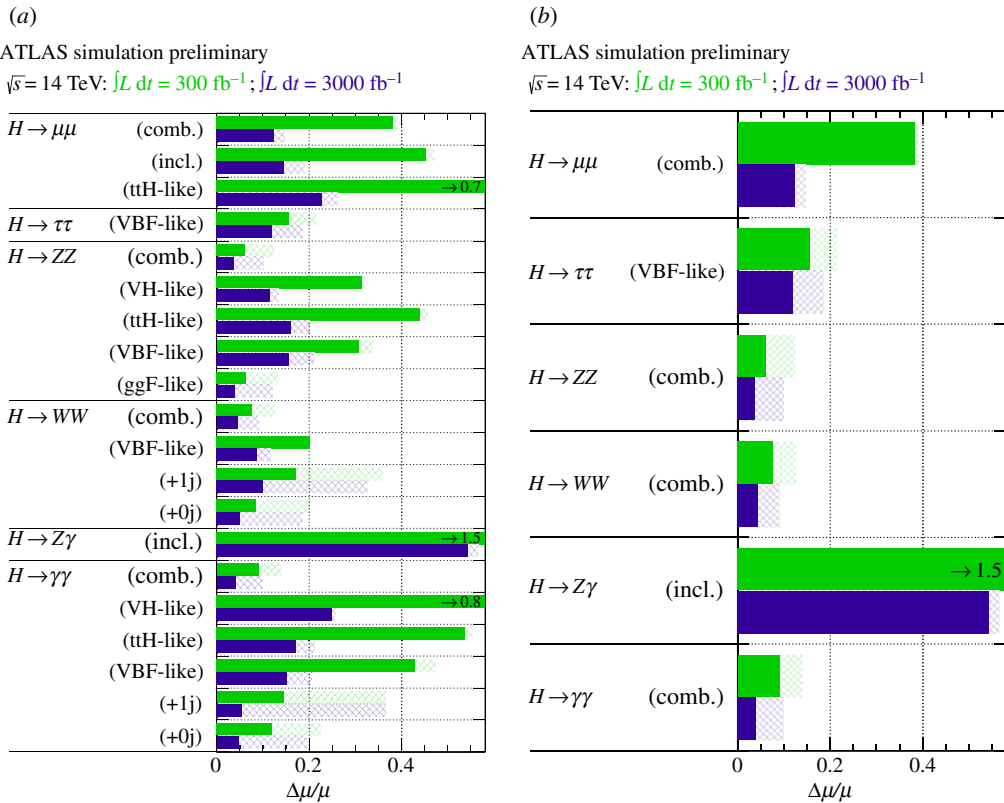


**Figure 10.** Signal strength uncertainty evaluated by ATLAS. The lighter grey/green bars show the expectation for  $300 \text{ fb}^{-1}$  and the darker grey/blue bars for  $3000 \text{ fb}^{-1}$ . The additional contribution from theoretical uncertainties is shown with the hatching. (a) Different production modes for each final state and (b) combined production modes. (Online version in colour.)

**Table 3.** Signal strength precision (in per cent) for ATLAS, where the range refers to results without/with theory uncertainty, and for CMS where the range is for the two error scaling scenarios.

$L(\text{fb}^{-1})$	exp.	$\gamma\gamma$	$WW$	$ZZ$	$bb$	$\tau\tau$	$Z\gamma$	$\mu\mu$
300	ATLAS	[9, 14]	[8, 13]	[6, 12]	n.a.	[16, 22]	[145, 147]	[38, 39]
	CMS	[6, 12]	[6, 11]	[7, 11]	[11, 14]	[8, 14]	[62, 62]	[40, 42]
3000	ATLAS	[4, 10]	[5, 9]	[4, 10]	n.a.	[12, 19]	[54, 57]	[12, 15]
	CMS	[4, 8]	[4, 7]	[4, 7]	[5, 7]	[5, 8]	[20, 24]	[14, 20]

All the different production modes can be observed for the  $ZZ$  and  $\gamma\gamma$  final states. In the case of the two sets of results from ATLAS, some uncertainties cancel out when combining the production modes to give the best possible precision on each decay mode; for example, the zero and one jet rates for  $H \rightarrow \gamma\gamma$  are anti-correlated. The CMS predictions are provided for the more pessimistic scenario 1 (present systematic uncertainties) and the more realistic/optimistic scenario 2 (systematic uncertainties scale with luminosity and theoretical errors divided by two). The signal strength precisions are listed in table 3. The dominant decay modes are measured to 4–5% precision, with 10–20% for the rare modes.

### (c) Interpretation as coupling scale factors

The experiments measure the product of the cross section (which measures the probability of producing a Higgs boson by the different mechanisms) times the branching ratio (which



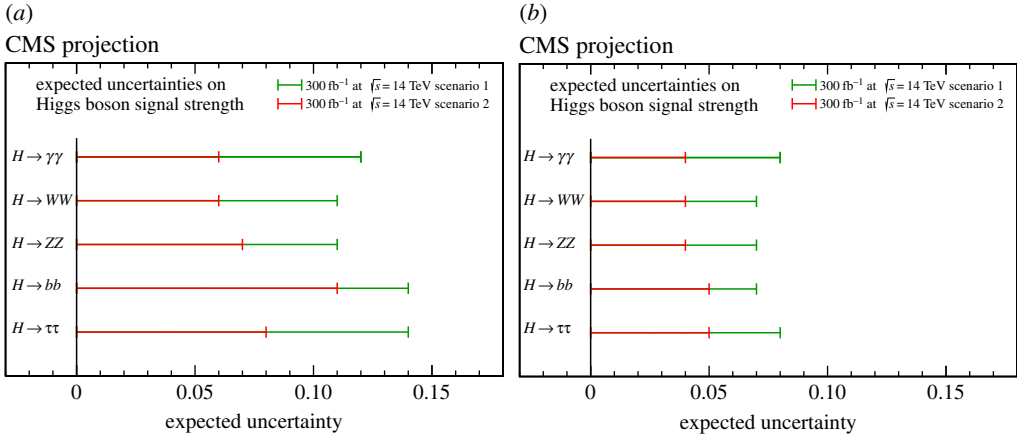


**Figure 11.** Signal strength uncertainty evaluated by CMS for 300 fb<sup>-1</sup> (a) and 3000 fb<sup>-1</sup> (b). In each case, the longer bars correspond to scenario 1 and the shorter bars to scenario 2. (Online version in colour.)

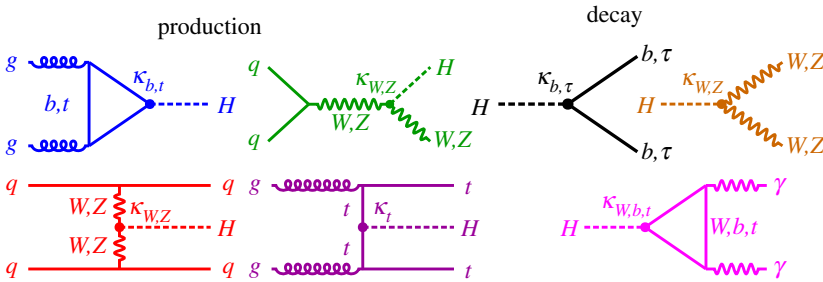


**Figure 12.** Diagrams illustrating production and decay of the Higgs boson in the standard model. (Online version in colour.)

gives the fraction of times the Higgs boson decays into a specific final state). The Standard Model production and decay processes are illustrated in figure 12. The interpretation of the measurements in terms of the Higgs couplings to other particles is model dependent and is performed in terms of the ratios,  $\kappa$ , of the fitted couplings to the Standard Model expectations. The cross-section times branching ratio for an initial state  $i$  and final state  $f$  is given by

$$\sigma \cdot Br(i \rightarrow H \rightarrow f) = \frac{\sigma_i \cdot \Gamma_f}{\Gamma_H}. \tag{3.1}$$

The total width of the Higgs boson,  $\Gamma_H$  is too narrow to measure, and the coupling fits assume that there are no additional invisible modes. Constraints on the rate of invisible decays can be made from data, but are not accounted for here. Predictions of the precision of the rate to charm quarks, and in the case of ATLAS to bottom quarks, are not yet available, so they are assumed to scale with the rate to  $\tau$ -leptons. Lastly, a choice can be made for the gluon and photon couplings to the Higgs boson. In the Standard Model, these are via loops, so depend on the couplings to the top and bottom quark, and for the photon to the  $W$  boson. However, in some models there could be additional heavy particles in the loops, in which case the gluon and photon can be given their own coupling scale factors,  $\kappa_g$  and  $\kappa_\gamma$ , which vary independently allowing for unknown additional effects.

Many possible coupling fits have been explored. One of the simplest is a two parameter fit which assumes that any deviation from the Standard Model is the same for the vector bosons,  $W$  and  $Z$ , and for all the fermions. This tests the structure of the theory, which gives mass to the

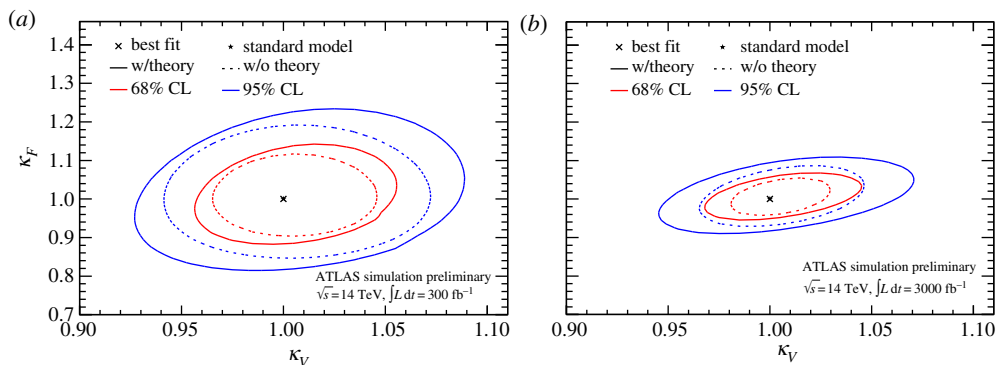


**Figure 13.** (a,b) ATLAS predictions for a two parameter fit with independent scaling for vector boson and fermion couplings. (Online version in colour.)

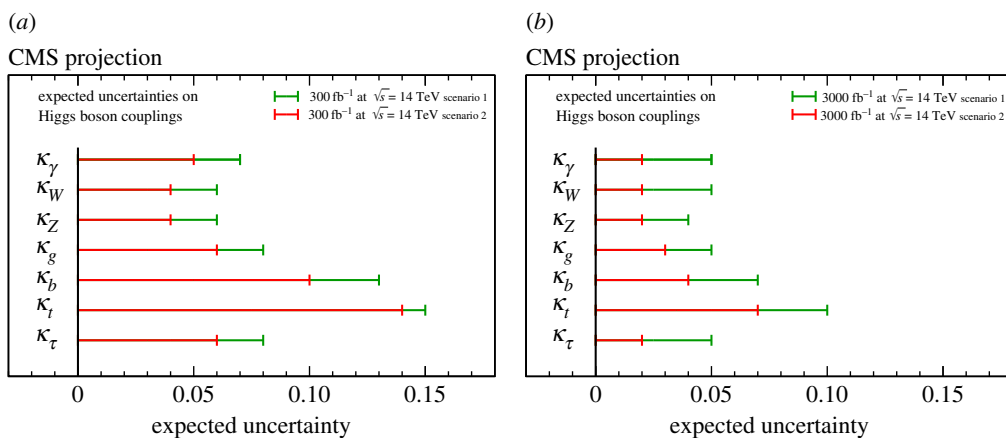


**Figure 14.** (a,b) Expected uncertainties in Higgs coupling scale factors from a generalized fit from CMS. (Online version in colour.)

**Table 4.** The precision in coupling scale factors (in per cent) from the generalized fits.

$\text{fb}^{-1}$	exp.	$\kappa_\gamma$	$\kappa_W$	$\kappa_Z$	$\kappa_g$	$\kappa_b$	$\kappa_t$	$\kappa_\tau$	$\kappa_{Z\gamma}$	$\kappa_{\mu\mu}$
300	ATL.	[8, 13]	[6, 8]	[7, 8]	[8, 11]	n.a.	[20, 22]	[13, 18]	[78, 79]	[21, 23]
	CMS	[5, 7]	[4, 6]	[4, 6]	[6, 8]	[10, 13]	[14, 15]	[6, 8]	[41, 41]	[23, 23]
3000	ATL.	[5, 9]	[4, 6]	[4, 6]	[5, 7]	n.a.	[8, 10]	[10, 15]	[29, 30]	[8, 11]
	CMS	[2, 5]	[2, 5]	[2, 4]	[3, 5]	[4, 7]	[7, 10]	[2, 5]	[10, 12]	[8, 8]

bosons and fermions by different mechanisms. As shown in figure 13, the HL-LHC brings an improvement of about a factor two, in particular if the theoretical uncertainties can be reduced.

In a more generalized coupling fit, the photon, gluon,  $W$ ,  $Z$  and the heavy fermions each have their own scale factor. The precision predicted by CMS is shown in figure 14, and the comparison between the ATLAS and CMS expectations is shown in table 4. There are some differences due to the fact that ATLAS has not yet released a prediction for the rate of  $H \rightarrow b\bar{b}$ . The systematic uncertainties partly cancel when taking ratios of coupling scale factors, and the model dependence is reduced. This is shown in table 5, where there is better agreement between

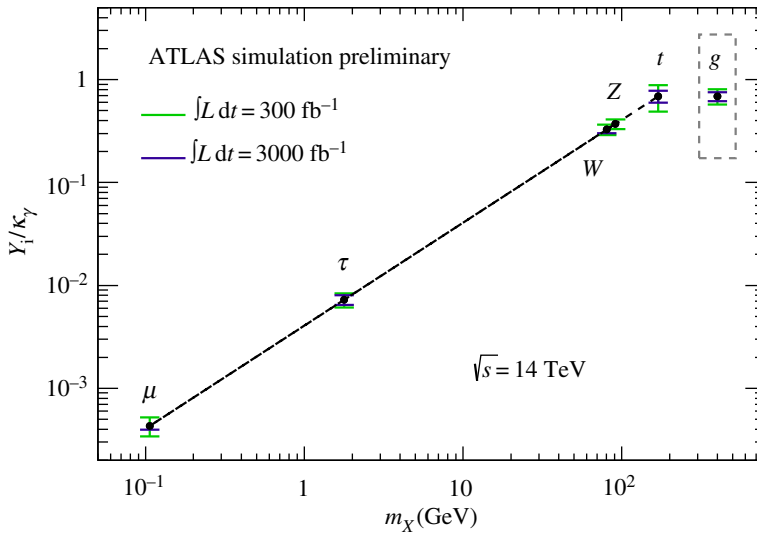


**Figure 15.** Coupling scale factors scaled by the particle masses, displayed as a function of particle mass. (Online version in colour.)

**Table 5.** The precision (in per cent) achieved in coupling ratios from the generalized fits.

fb <sup>-1</sup>	exp.	$\frac{\kappa_g \cdot \kappa_Z}{\kappa_H}$	$\frac{\kappa_\gamma}{\kappa_Z}$	$\frac{\kappa_W}{\kappa_Z}$	$\frac{\kappa_B}{\kappa_Z}$	$\frac{\kappa_\tau}{\kappa_Z}$	$\frac{\kappa_Z}{\kappa_\gamma}$	$\frac{\kappa_t}{\kappa_\gamma}$	$\frac{\kappa_H}{\kappa_Z}$	$\frac{\kappa_{Z\gamma}}{\kappa_Z}$
300	ATL.	[3, 6]	[5, 11]	[4, 5]	n.a.	[11, 13]	[11, 12]	[17, 18]	[20, 22]	[78, 78]
	CMS	[4, 6]	[5, 8]	[4, 7]	[8, 11]	[6, 9]	[6, 9]	[13, 14]	[22, 23]	[40, 42]
3000	ATL.	[2, 5]	[2, 7]	[2, 3]	n.a.	[7, 10]	[5, 6]	[6, 7]	[6, 9]	[29, 30]
	CMS	[2, 5]	[2, 5]	[2, 3]	[3, 5]	[2, 4]	[3, 5]	[6, 8]	[7, 8]	[12, 12]

the two experiments. The HL-LHC yields a factor 2 to 3 improvement in the coupling ratio determinations, and a precision of 2–3% can be achieved in the main channels if systematic uncertainties are under control.

An alternative way of displaying the coupling scale factors is to add the mass dependence explicitly, as shown in figure 15, which plots the mass scaled ratio

$$\frac{Y_i}{\kappa_\gamma} = \frac{\kappa_i \cdot m_i}{v} \cdot \frac{1}{\kappa_\gamma}, \quad (3.2)$$

as a function of the particle mass,  $m_i$ . In future, this kind of plot will reveal whether the couplings follow the trend predicted by the Standard Model.

#### (d) Direct and indirect searches for physics beyond the standard model

The prospects for finding new physics in the Higgs sector beyond the Standard Model have also been studied [12–14]. Many models which extend the Standard Model, such as supersymmetry, require more Higgs bosons. In supersymmetry, there are three neutral ( $h, H, A$ ) and two charged ( $H^+, H^-$ ) bosons resulting from a two Higgs doublet model. Figure 16a shows possible signals for a heavy Higgs boson  $H \rightarrow ZZ$ , compared with the rate of background processes. Direct searches can be complemented by constraints from coupling fits. For example, if the 125 GeV Higgs boson (which is usually the lower mass  $h$  in this kind of model) looks very like the Standard Model Higgs boson, it rules out various options in the theory. This is illustrated in figure 16b, as a function of two parameters,  $\alpha$  and  $\beta$ . If the couplings are measured to be consistent with the

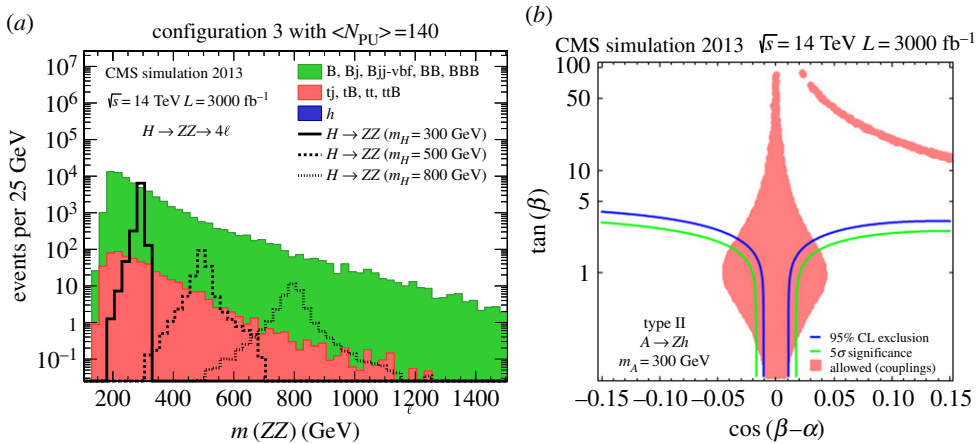


**Figure 16.** Trial heavy  $H \rightarrow ZZ$  signals compared with the expected background (a) and a comparison of constraints from coupling fits compared with the sensitivity of a specific direct search (b). (Online version in colour.)

Standard Model, they constrain these parameters to fall in the shaded region, while a direct search for the decay  $A \rightarrow Zh$ , which depends on the assumed mass of the  $A$ , would be sensitive to a complementary region.

## 4. Conclusion

The European Strategy for particle physics is that Europe's top priority should be exploitation of the full potential of the LHC, including the high-luminosity upgrade. The accelerator and the experiments have a well-defined upgrade programme, and the baseline Phase II detector designs allow the full physics potential to be achieved with 10 times the original design luminosity. The HL-LHC will investigate the 125 GeV Higgs boson in detail, with precise measurements of its couplings and sensitivity to rare processes. In addition, searches will continue for evidence of a more complex Higgs sector. The LHC, ATLAS and CMS have a long and productive future ahead.

**Acknowledgement.** I thank the organizers, John Ellis, David Charlton and Tejinder Virdee, for inviting me to this very enjoyable meeting, which celebrated the 50 year history of the Higgs boson, and then looked beyond. Thanks to colleagues in the ATLAS and CMS Collaborations for the many studies of the detector upgrades and physics prospects for future LHC running.

## References

1. *Accelerating science and innovation: societal benefits of European research in Particle Physics*, CERN-Brochure-2013-004-Eng. See <http://cds.cern.ch/record/1551933>.
2. ATLAS Collaboration. *ATLAS insertable B-layer technical design report*, CERN-LHCC-2010-013. See <http://cds.cern.ch/record/1291633>.
3. CMS Collaboration. *CMS technical design report for the pixel detector upgrade*, CERN-LHCC-2012-016. See <http://cds.cern.ch/record/1481838>.
4. ATLAS Collaboration. *New small wheel technical design report*, CERN-LHCC-2013-006. See <http://cds.cern.ch/record/1552862>.
5. CMS Collaboration. *CMS technical design report for the phase 1 upgrade of the hadron calorimeter*, CERN-LHCC-2012-015. See <http://cds.cern.ch/record/1481837>.
6. ATLAS Collaboration. *Letter of intent for the phase-II upgrade of the ATLAS experiment*, CERN-LHCC-2012-022. See <http://cds.cern.ch/record/1502664>.
7. CMS Collaboration. *CMS phase 2 upgrade: preliminary plan and cost estimate*, CERN-RRB-2013-124. See <https://cds.cern.ch/record/1605208/>.

8. CMS Collaboration. *Studies of the performances of the  $H \rightarrow ZZ \rightarrow 4\mu$  analysis with the CMS phase II detector upgrade*, CMS-PAS-FTR-13-003. See <https://cds.cern.ch/record/1607076>.
9. ATLAS Collaboration. *Projections for measurements of Higgs boson cross sections, branching ratios and coupling parameters with the ATLAS detector at a HL-LHC*, ATL-PHYS-PUB-2013-014. See <https://cds.cern.ch/record/1611186>.
10. CMS Collaboration. *CMS at the high-energy frontier contribution to the update of the European Strategy for Particle Physics*, CMS-NOTE-2012-006. See <https://cds.cern.ch/record/1494600>.
11. ATLAS Collaboration. *Performance assumptions based on full simulation for an upgraded ATLAS detector at a high-luminosity LHC*, ATL-PHYS-PUB-2013-009. See <https://cds.cern.ch/record/1604420>.
12. ATLAS Collaboration. *Sensitivity to new phenomena via Higgs couplings with the ATLAS detector at a high-luminosity LHC*, ATL-PHYS-PUB-2013-015. See <https://cds.cern.ch/record/1611189>.
13. ATLAS Collaboration. *Beyond-the-Standard-Model Higgs boson searches at a high-luminosity LHC with ATLAS*, ATL-PHYS-PUB-2013-016. See <https://cds.cern.ch/record/1611190>.
14. CMS Collaboration. *Performance studies on the search for 2HDM neutral Higgs bosons with the CMS phase-II detector upgrades*, CMS-PAS-FTR-13-024. See <https://cds.cern.ch/record/1607086>.